Prabha Materials Science Letters
Vol. 3, No. 1, 60-76, 2024
https://doi.org/10.33889/PMSL.2024.3.1.004

Ram Arti Publishers

Mechanical and Tribological Characterization of Green Composite Fabricated by Wheat Flour and Wheat Straw

Sandeep Kumar Yadav
Department of Mechanical Engineering,
Malaviya National Institute of Technology Jaipur, Jaipur, Rajasthan, India.
E-mail: sandeepsky666@gmail.com

Pankaj Kumar Gupta
Department of Mechanical Engineering,
Malaviya National Institute of Technology Jaipur, Jaipur, Rajasthan, India.
Corresponding author: pankaj.mech@mnit.ac.in

Tapas Bajpai
Department of Mechanical Engineering,
Malaviya National Institute of Technology Jaipur, Jaipur, Rajasthan, India.
E-mail: tapas.mech@mnit.ac.in

(Received on September 13, 2023; Revised on January 1, 2024; Accepted on January 11, 2024)

Abstract
The excessive use of traditional plastic polymers has elevated environmental concerns. These polymers are extremely difficult to dispose off. It takes a long time for plastics to disintegrate. These plastics enter into river water through several channels, and for a considerable amount of time, it flows with the stream. Numerous marine creatures get sick after ingesting the trash and animals on the ground. Therefore, an effort is made for such a green composite which do not harm the creatures and animals. A green composite material was fabricated by compression molding using wheat flour (WF) as a matrix and wheat straw (WS) as a reinforcement. Both materials are natural and digestible for living beings. WS was lighter than WF, so the addition of WS made the composite lighter. A poly-lactic acid (PLA) coating was done over the surface of the WF-WS composite to make it water resistant and wear resistant. The pin on disc wear test was performed to get the specific wear rate of the composite. The air jet erosion was also carried out to know the erosion value of the composite. The thermo-gravimetric analysis was performed to investigate the thermal stability of the composite in order to ensure the use of the composite up to 200° C. It was found that the addition of WS fibers in the composite increased thermal stability. The scratch test was conducted to find out the strength of the 1 mm thickness coating. The WF-WS composite with PLA coating can be used in non-load bearing components and light weight applications. It can also be used for eco-friendly food packaging materials.

Keywords- Wheat straw (WS), Wheat flour (WF), Poly-lactic acid (PLA), Green composite.

1. Introduction

Composite materials are made from two or more constituent elements having distinct physical or chemical characteristics. Composite materials are less expensive, stronger, lighter and more durable than conventional materials**.** The first artificial fiber reinforced plastic was fabricated from fiber glass and bakelite in 1935 (Composite *Materials*, n.d.). The invention of plastic was a revolutionary step in the development of human civilization. The disposal of plastic is a challenge due to its non-biodegradable nature. Producing traditional plastics requires 65% more energy and emits 30-80% more greenhouse gases than bioplastic (Owens corning milestones, 2017). Convention fiber reinforcement plastics (FRPs) have problem of disposal after the completion of life cycle of composite. For reducing the use of these plastics, other suitable option needed such as green composites (Ben et al., 2013). FRPs has become increasingly popular in replacing traditional materials due to its exceptional strength-to-weight ratio (Begum et al.,

2020). There were about 322 million tons of plastic produced worldwide in 2015 with a 3.5% increase from 2014 (Mangaraj et al., 2019). The production of plastic increased from 1.5 million tons in the 1950s to about 400 million tons in 2018 (Taib et al., 2023). The European Union (EU) vision, which was unveiled in January 2018, sets a goal of more environmentally friendly plastic industries by 2030. This strategy promotes the use of biodegradable polymers instead of conventional plastics. The pollution increasing throughout the world is the greatest concern for the environment. In 2020, there were 400 million tons of plastics produced globally. It is estimated that in the year 2050, the production of plastic will reach 1100 million tons (Plastic, n.d.). The market of composite fabricated by epoxy and petroleum-based filaments will reach about $130.83 billion by 2024 (Eldeeb et al., 2022). Plastic collecting and recycling are primarily inefficient due to the complexity involved in cleaning and classifying post-consumer plastics for efficient reuse (Eldeeb et al., 2022). The majority of plastic manufactured has not been recycled and instead ends up in landfills or pollutes the environment (Jem and Tan, 2020). In industrialized economies, around 33% plastic is used for wrapping, and about a similar amount is utilized in structures for things like plumbing and piping (Tobis et al., 2018.).

The matrix and reinforcement are selected according to the required properties of the composite, which can vary according to the matrix and reinforcement. The utilization of fiber hybridization has addressed numerous difficulties in the realm of FRPs. However, the main hurdle that persists in the manufacturing of FRPs is finding cost-effective and environmentally sustainable materials (Ismail et al., 2022). Green composites are suitable alternatives as sustainable materials. The rigidity of the green composite depends on the amount of filler content (Scaffaro et al., 2009a). It was observed that rigidity increases as the filler content is increased and other properties also change with filler content (Morreale et al., 2008a). It was discovered that the filler content has the greatest impact on elastic modulus, even though matrix pretreatment and mixing speed also appeared to have an effect (Morreale et al., 2008b). The rigidity significantly increased when wood flour was used, but ductility decreased (Scaffaro et al., 2009b). There is a wide field of applications for green composites i.e. biomedical applications such as tissue engineering, the packaging industry, the automobile industry, the aerospace industry, electrical and electronics applications (Alvarez et al., 2005, 2006). Engineered cementitious composites (ECCs) have the property to enhance ductility and toughness (Altwair et al., 2012). Green composites have the potential to partially replace cement for reinforced cement concrete (RCC). Palm oil fuel ash (POFA) is one example that can partially replace cement (Kim et al., 2003). Researchers conducted studies on polymer/ carbon nano tube (CNT) composites with the aim of enhancing the soundproofing capabilities of polymers (Lee et al., 2008). Wheat straw is a byproduct of wheat farming. The use of wheat straw fibers in bio composites can improve mechanical properties, reduce cost, and provide an environment friendly alternative to traditional synthetic fibers (Jiang et al., 2020). Another application of wheat straw as a matrix is in the production of paper. The resulting paper had good strength and printability, indicating that wheat straw can be used as a viable alternative to traditional wood pulp in paper production (Montaño-Leyva et al., 2013).

Wheat flour is one of the most important ingredients in several food industries. It is widely used as a matrix in different food items. Wheat flour is obtained by milling wheat grains. Wheat flour is the composition of various components such as starch (70-75%), protein (7-15%), lipids, fiber, and minerals (Shewry, 2009). Wheat flour is a good matrix due to possessing unique physical, chemical, and rheological properties. Particle size, shape, and distribution of wheat flour play an important role to determine the texture and structure of a product. The chemical properties of wheat flour, such as its composition and reactivity, affect the functional properties of the flour (Hrušková et al., 2001). Wheat gluten, a plant-derived protein, has gained significant interest as a bio-based plastic due to its utilization as a byproduct in bioethanol and cereal processing industries. This attention stems from its recent recognition as a viable material for bio-based plastic applications (Mensah et al., 2022). The gluten proteins found in wheat flour form a viscoelastic

network that traps the carbon dioxide produced during fermentation (Litwinek et al., 2016). This comprehensive review leads to fabrication and investigations on green composites in subsequent sections. In this research work, wheat flour (WF) with water was taken as matrix and wheat straw (WS) was taken as reinforcement. PLA coating was applied over the fabricated WF-WS composite.

2. Materials and Methods

The matrix and reinforcement materials used in green composite with fabrication technique are detailed in the following subsections.

2.1 Materials

The wheat flour was obtained by milling of wheat grains as shown in Figure 1(a). Wheat grains possess an ample amount of gluten protein that creates a viscoelastic network. The wheat straw was obtained from agricultural wastes of wheat forming as shown in Figure 1(b). Wheat straw was pale yellow in colour and it was light in weight. The flash point of wheat straw lies between 180° C to 220° C depending on specific conditions. Poly-lactic acid (PLA) was taken for the purpose of coating which is shown in the form of wire in Figure 1(c). The PLA used in this composite was having 1.75 mm diameter. Its melting point was 170°C.

(a) (b) (c)

Figure 1. (a) Wheat flour, (b) Wheat straw, (c) Wire pool of PLA.

2.2 Fabrication of WF-WS Composite

The mold was cleaned with tissue paper. After cleaning the mold, a plastic was placed on the surface of the mold so that it avoids the adhesion of the composite to the mould surface during ejection. Now, the material was prepared. Wheat straw was taken in different proportions (5%, 10% and 15%) as given in Table 1 and a fixed quantity (100 ml) of water was taken. Wheat flour, and wheat straw were put into a mixture grinder with water, and it was mixed at 20000 rpm for 10 minutes so that wheat straw could be homogeneously distributed throughout the composite. The mixture of WF and WS was placed into the mold. The pressure was applied on the composite with the help of a plunger so that the material could take the shape of the mold. After 10 minutes, the composite was ejected from the mould. Now, it was baked in the oven at 50 °C for 30 hrs. Here, the WF-WS composite was prepared. After the fabrication of the composite, the PLA coating was done over the composite. PLA wire was melted over the surface of the composite, and it form a layer on the surface.

Table 1. Sample composition of WF-WS composite.

Sample Name	WS
S1	5 %
S2	10 %
S3	15 %

2.3 Characterization Methods

The fabricated composite was tested by different methods to characterize it mechanically and tribologically. These tests were used to investigate the properties such as wear resistance, erosion resistance, thermal stability, etc. of composite. The details of the test are given in the below subsections.

2.3.1 Density and Void Test

A material's density is a measurement of mass present in a specific volume of that material. In other words, a substance's mass per unit volume is density. A substance can be recognized by its density (Julias, n.d.). Higher-density materials typically have stronger and long-lasting properties than lower density materials. This is because a denser material is harder to deform or break because it has more mass per unit volume. The density of the composite can be calculated by the following formula:

$$\rho_c = \frac{w_m + w_f}{\frac{w_m}{\rho_m} + \frac{w_f}{\rho_f}} \quad (1)$$

where,
ρ_C = Density of the composite,
W_m = Weight fraction of matrix,
W_f = Weight fraction of fiber,
ρ_m = Density of the matrix,
ρ_f = Density of fiber.

Voids in a composite material are essentially gaps that can reduce the material's strength and stiffness. The void formation can occur during the manufacturing process for a number of reasons, including insufficient matrix and fiber mixing, poor curing, and the use of inferior materials (Schwartz, 1992). A lack of compaction during the manufacturing process can result in spaces between the fibers and matrix, which can also contribute in the presence of voids. Voids are obtained in composite by the difference of theoretical and experimental density. Generally, in these cases, the theoretical density is greater than the experimental density.

Voids can be calculated by the following equation:

$$v_c = \left[1 - \frac{\rho_a}{\rho_{th}}\right] \quad (2)$$

where,
V_c = Void content in composite,
ρ_a = Actual density of composite,
ρ_{th} = Theoretical density of composite.

2.3.2 Water Absorption Test

The water absorption test is a technique used to find out the porosity and permeability of a material. During the test, a dry sample of the material is submerged in water for a predetermined period of time. The weight gain by the material's pores due to the absorption of water is measured (Muñoz et al., 2015). The water

absorption test is based on the principle of capillary action, which describes how a liquid flow through small spaces as a result of the cohesive and adhesive forces between the molecules of the liquid and the solid surfaces (Nyambo et al., 2011).

The formula for calculating the water absorption percentage is:

$$\text{Water absorption } (\%) = \left[\frac{W2-W1}{W1}\right] * 100 \quad (3)$$

where,
W1 = Initial dry weight of the specimen,
W2 = Weight of the specimen after immersion in water.

2.3.3 Wear Test

It is a tribological test used to determine the friction and wear properties of materials on pin-on discs. During the test, a pin specimen was slide against a rotating disc while being subjected to control load, speed, and temperature (Li et al., 2015). In the pin-on-disc test apparatus, the disc is made of a harder material than the specimen (Pin on Disk Test, n.d.). To simulate various contact conditions, the pin's dimensions and surface finish can be changed. The specimen can be taken in the form of a cylindrical, cuboidal, or conical shape. In this experiment, the specimen was taken in cuboidal form having dimensions $12mm \times 5mm \times 5mm$.

The specific wear rate can be calculated as:

$$w_{sp} = \frac{\Delta m}{\rho t v F} \quad (4)$$

where,
w_{sp}= Specific wear rate (mm^3/m),
Δm= Change in mass,
ρ = Density of composite,
t = time in sec,
v = Velocity (m/sec),
F= Normal load.

2.3.4 Erosion Test

Air jet erosion test is a technique used to evaluate the resistance of materials to erosion due to high-velocity air streams. Air jet erosion test simulates the erosive effects of dust, sand, and other abrasive particles present (Desale et al., 2006). In the air jet erosion test, a high-speed air stream is directed at a specimen surface from a fixed angle and distance, and the mass loss or volume loss of the specimen was measured over a predetermined period of time (Balamurugan et al., 2020).

The erosion value can be calculated as:

$$Ev = \frac{Loss\ in\ volume\ of\ specimen}{Erodant\ consumed} \quad (5)$$

2.3.5 Thermogravimetric Analysis (TGA)

Thermogravimetric analysis (TGA) is a technique to study the thermal behaviour of materials (polymers, ceramics, metals, composites, etc.) when these are kept under changes in temperature. It measures the change in mass of a sample as it is heated or cooled. This provides information about its thermal stability, decomposition, and reaction kinetics (Thermo-gravimetric analysis, n.d.). When the sample goes through

the temperature change, changes in the mass of the sample due to various phenomena such as decomposition, vaporization, oxidation, absorption, sublimation, etc., are investigated by TGA. The basic setup of a TGA instrument consists of a furnace where the sample can be heated, a balance that measures the mass, and a temperature controller that regulates the furnace temperature. The sample is placed in a crucible, which is then placed on the balance. When the temperature of the furnace is increased or decreased, the balance records changes in the mass of the sample (Liu and Yu, 2006).

2.3.6 Scratch Test

The scratch tester (TR-101) is a device used to find out the scratch resistance of materials. It is commonly used in industries such as automotive, aerospace, and coatings. The TR-101 consists of a diamond stylus to scratch the material's surface during the test. The stylus is mounted on an arm. This arm moves in a controlled manner across the material's surface. The scratch width and depth can be formed on the surface to simulate different types of scratches that the material may face in real-world applications (Technical specifications Test Setup Screen Test Graph Showing Normal Load And Tan-gential Force (Ft), n.d.). The scratch resistance of the material is obtained by measuring the force required to produce a visible scratch on the surface. The TR-101 can also be used to find out the adhesion of coatings by measuring the force required to delaminate the coating from the substrate (Perry, 1983).

3. Results and Discussion

3.1 Density and Void Content in WF-WS Composite

The actual and theoretical density was calculated as per Equation (1). Void content was calculated as per Equation (2) which are given in Figure 2 and Figure 3.

The actual density of the composite was found lesser than the theoretical density of the WF-WS composite as shown in Figure 2. The voids were considered during the calculation of actual density as given in Equation (1) while these voids were not considered in theoretical density (mass/volume) (Schwartz, 1992).

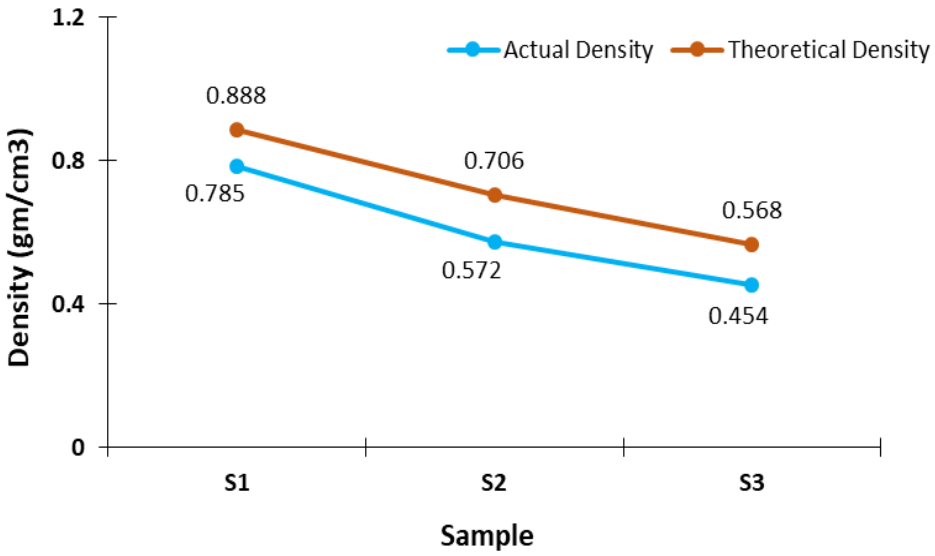

Figure 2. Actual and theoretical density of samples.

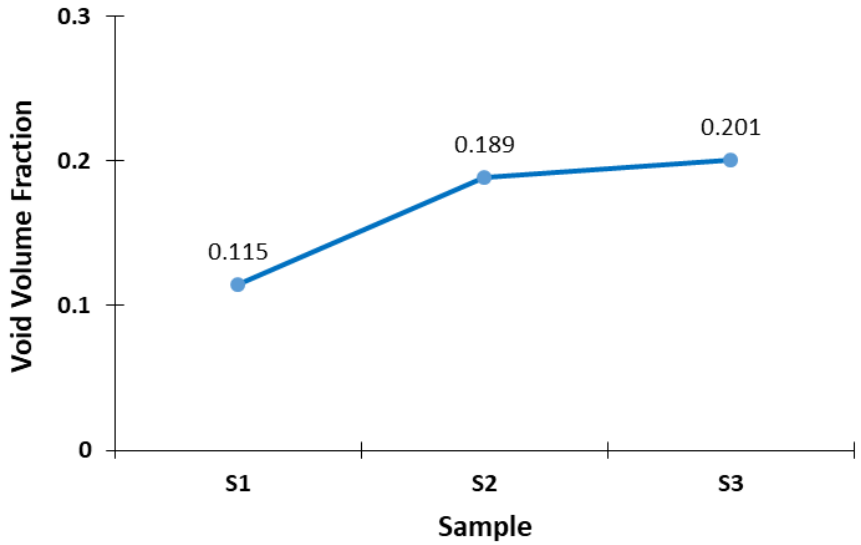

Figure 3. Void volume fraction of samples.

It was observed that the density of WF-WS composite decreased with an increase in WS content. The density of WS is lesser than the density of WF. Therefore, the increase in WS fibers in composite makes it lighter. The void content was increased as the WS percentage was increased in the composite as shown in Figure 3. The surface area of WS was increased by increasing the WS fibers in the composite. There was a lack of adhesion by WF to bind all WS fibers together in the composite and generating voids in the composite.

3.2 Effect of Water on WF-WS Composite

Composite materials can experience abnormal effects from water absorption. Wheat flour and wheat straw both have hydrophilic property in nature.

The water absorption by WF- WS composite was observed as shown in Figure 4. It was found that water absorbed by sample S2 was maximum. WF and WS both are hydrophilic in nature so water absorption by the composite may occur. WF showed more water absorption than WS due to the presence of more gluten protein. The WF fraction was maximum in sample S1 but there were relatively less voids available to hold the water molecules. So, the water absorption was minimum in sample S1 than other samples. In the case of sample S2, there was more WF and less WS as compared to sample S3. One fact should be noticeable that the more WS increases the voids in S3 but it cannot absorb the water molecules as much as WF. As the WF fraction was more in sample S2 and also enough voids were present to hold the water molecules, therefore sample S2 absorbed more water than sample S3.

It was seen that water absorption decreased as compared to uncoated composite samples after the PLA coating as shown in Figure 5. PLA had hydrophobic nature that's why it was selected for coating so that the water absorption could be reduced during use.

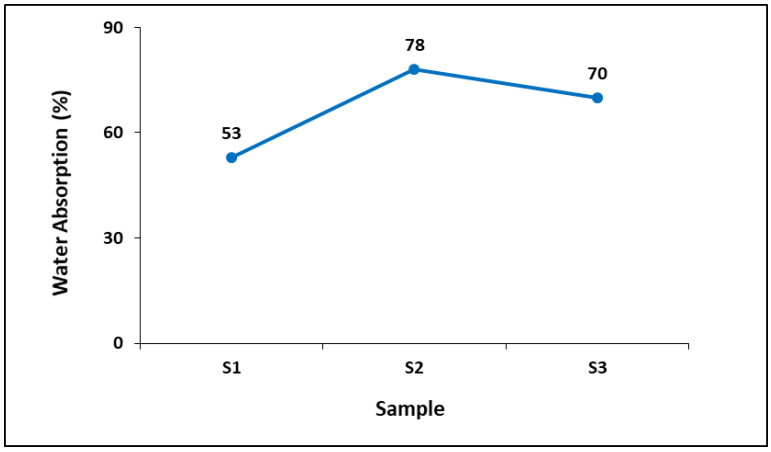

Figure 4. Water absorbed by WF-WS samples -non-coated.

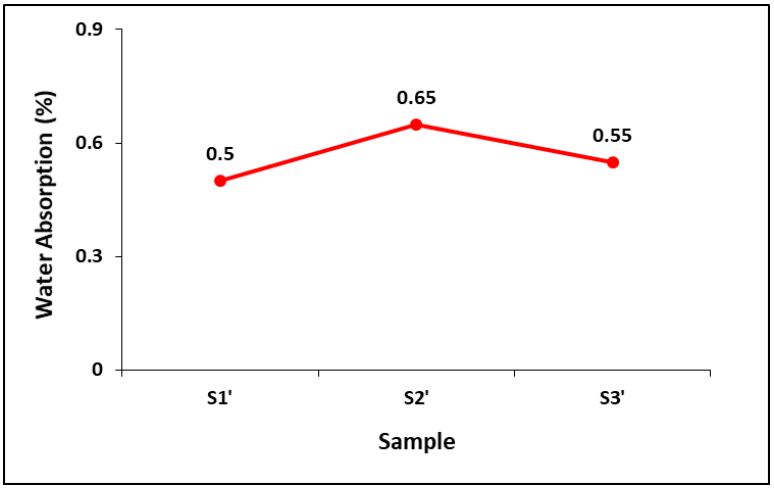

Figure 5. Water absorbed by PLA-coated WF-WS samples -PLA coated.

3.3 Specific Wear Rate of WF-WS Composite

The wear rate of the WF-WS composite was found by pin on disc test. The track radius was kept as 40 mm and the speed was maintained at 300 rpm for 10 minutes to perform the test. A 1 kg load was applied to the sample. The wear rate can be measured by the mass loss or volume loss of the pin over a specified sliding distance or time. The samples are shown in Figure 6. The specific wear rate of the WF-WS composite was calculated using Equation (4) which are shown in Figure 7 and Figure 8.

(a) (b)

Figure 6. Samples of pin on disc test (a) Non-coated (b) Coated.

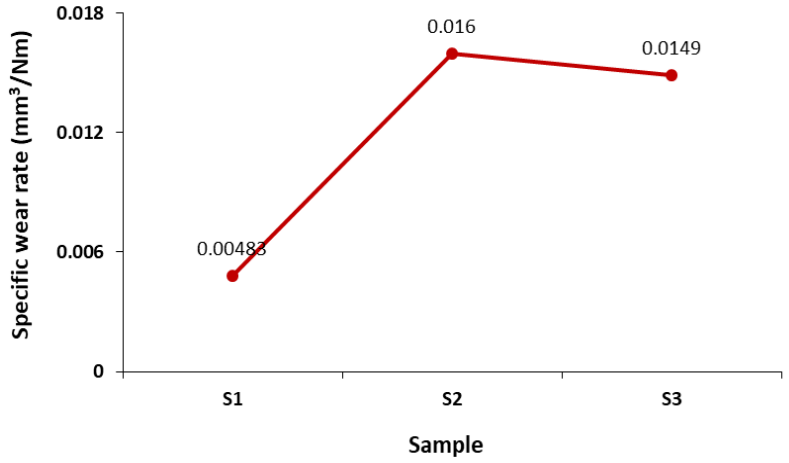

Figure 7. Specific wear rate of WF-WS samples-non-coated.

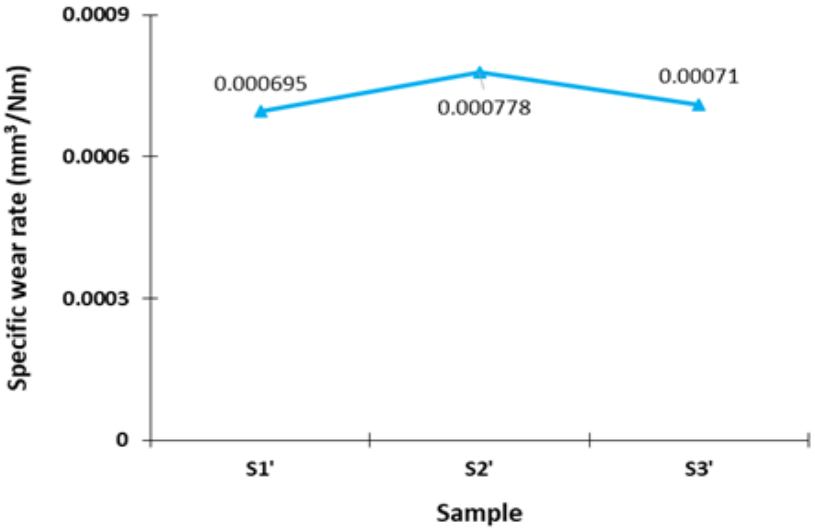

Figure 8. Specific wear rate of WF-WS samples -PLA coated.

It was observed that the wear rate was minimum in sample S1 as compared to other samples as shown in Figure 7. In sample S1, there was more amount of WF available to hold the WS fibers and provide good adhesion force. This sample had fewer voids and high density that decreased wear. The maximum wear rate was shown in S2. There was less amount of WF for holding the WS. Therefore, there is a weak binding force between WF and WS in sample S2. In the case of S3, there was less amount of WF available while WS was more in quantity. The fibrous nature of wheat straw provides robust structural integrity, contributing to its enhanced durability. Additionally, wheat straw fiber exhibits less abrasive properties compared to the finer particles of wheat flour, resulting in reduced friction and wear (Chand and Fahim, 2020). There was also weak binding force in sample S3 but WS was in the form of fiber and more wear resistive as compared to WF. That's why sample S3 showed lesser wear than sample S2.

The specific wear rate was reduced in PLA coated samples as shown in Figure 8. This depicted that PLA possessed good wear resistive properties.

3.4 Erosion Wear Analysis on WF-WS Composite

The erosion value of WF-WS composite was determined by an air jet erosion test. The sand of 50 µm was used as erodent material. The air jet pressure was set to 0.30 bar and the corresponding velocity was 30 m/s. The erodent discharge rate was set to 2 gm/min and the erodent was allowed to flow with the air stream for 10 minutes. The erosion values were calculated by Equation (5). The samples are shown in Figure 9 and Figure 10.

(a) 45^0 impact angle (b) 60° impact angle

Figure 9. WF-WS samples non-PLA coated for air jet erosion test (a) 45° impact angle (b) 60° impact angle.

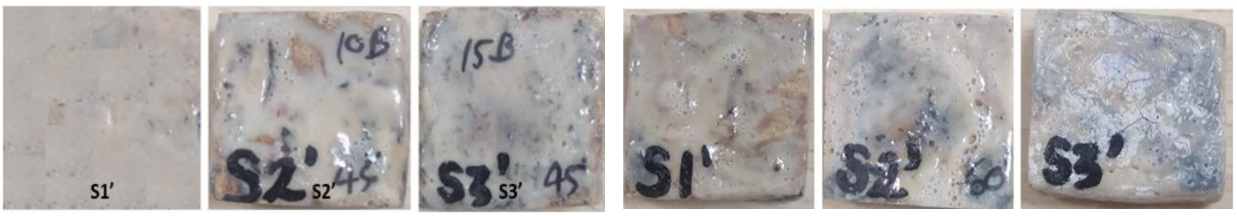

(a) 45° impact angle (b) 60° impact angle

Figure 10. WF-WS samples PLA coated for air jet erosion test (a) 45° impact angle (b) 60° impact angle.

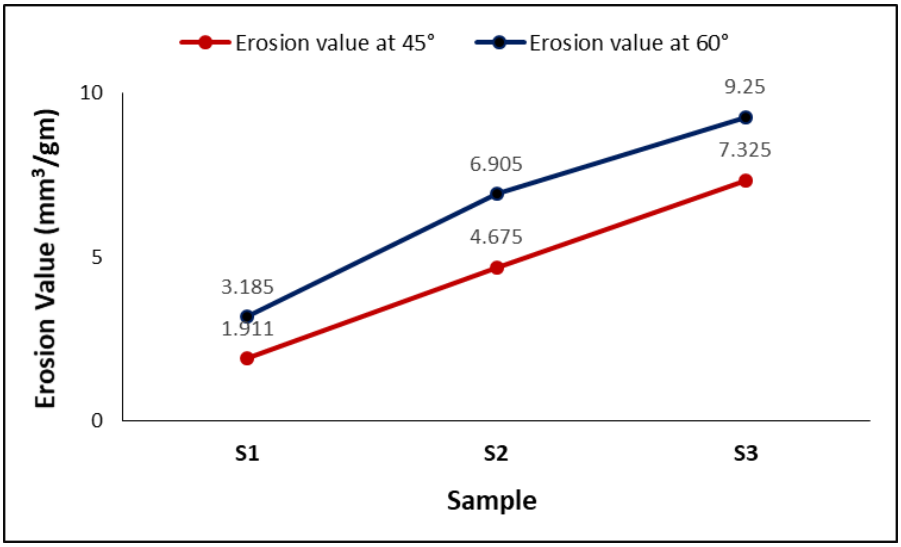

Figure 11. Comparison of erosion value of different WF-WS samples at 45° & 60°.

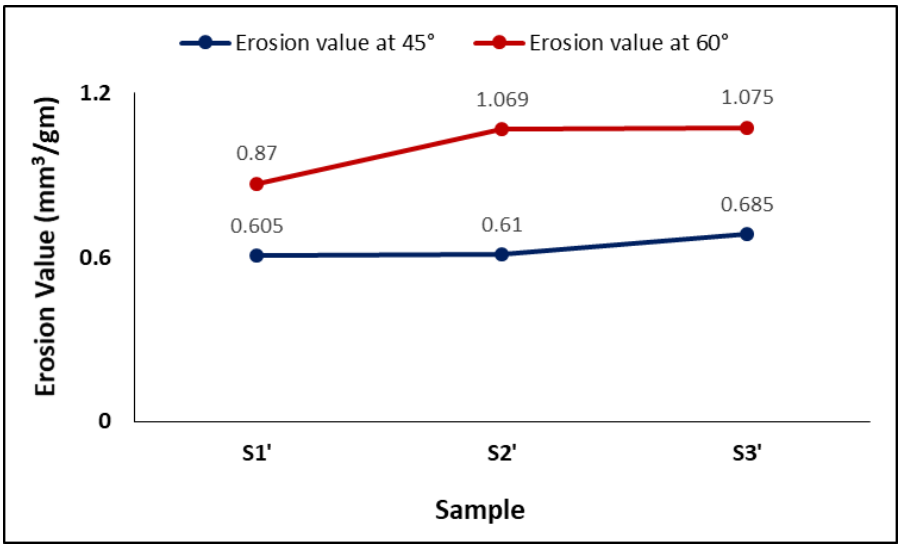

Figure 12. Comparison of erosion value of PLA coated WF-WS samples at 45° & 60°.

It was found that sample S3 showed the highest erosion value as compared to other samples for a particular impact angle as shown in Figure 11. It was due to the higher amount of voids available in the composite. Sample S3 had weak bonding and high void content between the matrix and reinforcement. The erosion value was significantly reduced after the PLA coating over the WF-WS composite as shown in Figure 12. It was observed from Figure 12 that PLA coating had good erosion resistive properties at the velocity of 30 m/s.

It was noticed that the erosion value for a particular sample at 60° was greater than 45°. Erosion was typically characterized by cutting and gouging of the surface at a low angle of incidence, while plucking and lifting of particles were predominant at higher angles of incidence (Yadav et al., 2022). Therefore, it was investigated that the mass loss in air jet erosion testing increased as the angle of incidence was increased. This was due to the fact that higher angles cause abrasive particles to strike the surface more obliquely and with lesser force than lower angles do. This caused less cutting and more surface material plucking. A greater amount of material might be plucked from the surface as a result of this action which increased the mass loss.

3.5 Thermo-Gravimetric Analysis (TGA)

Thermo-gravimetric analyzer STA 6000 (Perkin Elmer) was used to perform the TGA test. The temperature range was used from room temperature (27 °C) to 200 °C during the TGA test. The temperature rate was set 5 °C/min. There were three samples named S1, S2, and S3 considered for the test. Sample S3 showed less decomposition than S2 and S1 when the temperature was raised from 27 °C to 200 °C as indicated in Figure 13.

Sample S3 was found thermally more stable as compared to other samples. There was not so good interfacial bonding between the WF and WS even though sample S3 showed good thermal stability because WS had more thermal resistance than WF. The WS had cellulose, hemicellulose, lignin, etc. which were complex organic polymers and showed higher thermal stability. In contrast, WF had starch, proteins, and lipids. Starch and proteins can undergo thermal decomposition at relatively lower temperatures compared to cellulose and lignin. Lipids (fats and oils) present in wheat flour are also susceptible to thermal degradation. As a result, wheat flour tends to have lower thermal stability compared to wheat straw.

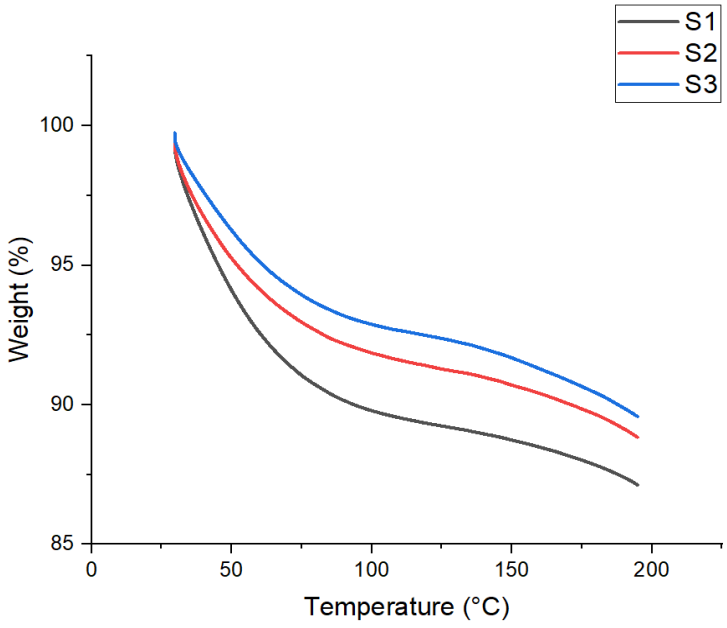

Figure 13. Thermo-gravimetric curves of samples.

3.6 Strength of PLA Coating on WF-WS Composite

The strength of coating shows the resistivity against the scratch load. The strength of the coating can be defined as the load required to fail the coating. A scratch test had been done to determine the adhesion of the coating. A scratch tester (TR-101) device was used to perform the test. Rockwell C type with nose radius 200 micron diamond indenter was used in Scratch tester (TR-101). Four scratches were selected during performing the test. These scratches contained 10N, 20N, 30 N, and 40 N loads respectively. The offset distance between two scratches was provided 1mm. The scratch length was provided 5 mm for all four scratches. The scratch velocity was set to 0.2 mm/sec. The sample after the scratch test are shown in Figure 14.

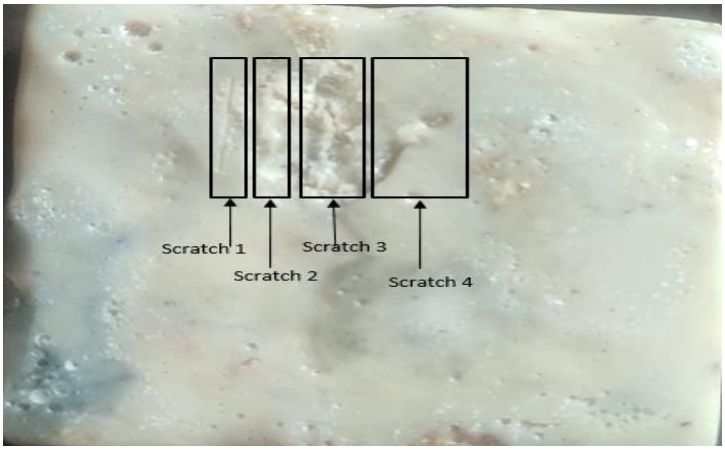

Figure 14. Sample after scratch test.

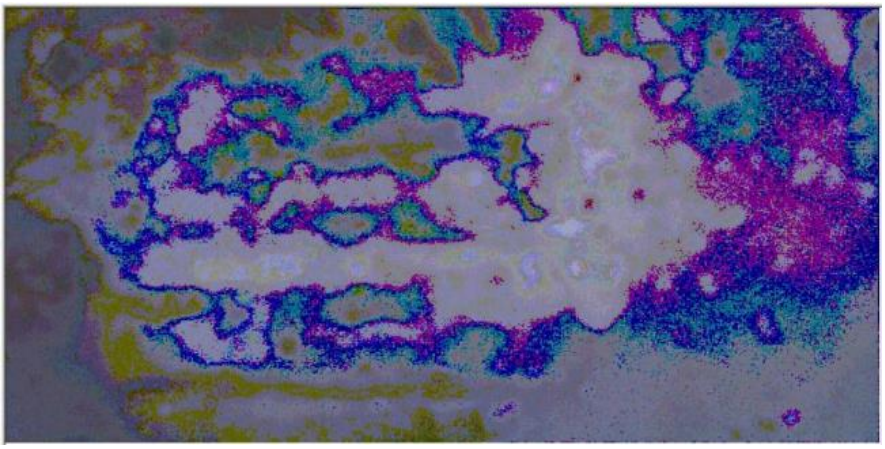

Figure 15. Infra-red image of coating by scratch tester.

It was found that the coating was able to sustain the scratch load of 10 N and 20 N but it showed failure at 30 N and 40 N. Figure 18 shows the infra-red image of the scratched sample. At the load of 30 N, the coating failed at 4.7 mm scratch length. The failure occurred at a very less scratch distance which was 0.5 mm at 40 N load as shown in Figure 15. The bonding between the coating and the composite substrate became insufficient to withstand the higher stress levels as the applied load increased beyond 20 N. This

caused the coating to fail, showing that its adhesion strength was surpassed, resulting in detachment or damage. The results obtained from Figure 15 showed that the coating was safe under 20 N loads.

4. Conclusions

The WF-WS composite was fabricated by manual compression method. The fabricated composite was characterized for mechanical and tribological properties. The following conclusions were observed after investigations.

- The density of WF-WS composite was decreased as the WS content increased in the composite. This happened because the density of WS was lower than WF.
- Sample S2 absorbed 78 % of water. But after the PLA coating, it was reduced to 0.65 %. The WF- WS composite is highly susceptible to water due to its hydrophilic nature which was reduced by PLA coating due to its hydrophobic nature.
- The specific wear rate of sample S1 was 0.00483 mm^3/N m and it was minimum among the other samples of WF-WS composite. It is attributed to good interfacial bonding between the WF and WS. It was further reduced to 0.000695 mm^3/N m after the PLA coating.
- The erosion value at 45° of sample S1 was 1.911 mm^3/gm. It was minimum among other compositions of WF-WS composite because it had good interfacial bonding and high density. It was further reduced to 0.605 mm^3/gm after the PLA coating.
- The erosion value at 60° of sample S1 was 3.185 mm^3/gm and it was also minimum among other compositions of WF-WS composite which was reduced to 0.87 mm^3/gm after the PLA coating.
- Sample S3 was more thermally stable as compared to the other two compositions. Sample S3 had more amount of WS fibers. WS fibers are more thermally stable than WF due to the presence of cellulose, hemicellulose, lignin, etc. Sample S3 showed 10% loss in mass as the temperature increased from 27°C to 200°C.
- The PLA coating over the WF-WS composite failed at 30 N load. The adhesion between PLA coating and composite substrate was unable to withstand the load above 20 N. Therefore, the PLA coating was safe under 20 N load with 1 mm thickness.

The potential applications of the WF-WS composite with PLA coating may be in non-load-bearing components, utensils and light weight packaging applications. One possible application for a WF-WS composite with a PLA coating is in the production of eco-friendly food packaging materials. The packaging produced from this composite could be used for food products like bread, pastries, snacks, etc.

Conflict of Interest

The authors have no conflicts to disclose.

Acknowledgments

The authors are thankful to the Department of Mechanical Engineering, Malaviya National Institute of Technology Jaipur, Jaipur, (Rajasthan) for carrying out this research work. The authors are also thankful to the reviewers for their valuable suggestions.

References

Altwair, N.M., Megat Johari, M.A., & Saiyid Hashim, S.F. (2012). Flexural performance of green engineered cementitious composites containing high volume of palm oil fuel ash. *Construction and Building Materials*, *37*, 518-525. https://doi.org/10.1016/j.conbuildmat.2012.08.003.

Alvarez, V., Vázquez, A., & Bernal, C. (2005). Fracture behavior of sisal fiber-reinforced starch-based composites. *Polymer Composites*, *26*(3), 316-323. https://doi.org/10.1002/pc.20103.

Alvarez, V., Vázquez, A., & Bernal, C. (2006). Effect of microstructure on the tensile and fracture properties of sisal fiber/starch-based composites. *Journal of Composite Materials*, *40*(1), 21-35. https://doi.org/10.1177/0021998305053508.

Balamurugan, K., Uthayakumar, M., Ramakrishna, M., & Pillai, U.T.S. (2020). Air jet erosion studies on Mg/SiC composite. *Silicon, 12*(2), 413-423. https://doi.org/10.1007/s12633-019-00148-y.

Begum, S., Fawzia, S., & Hashmi, M.S.J. (2020). Polymer matrix composite with natural and synthetic fibres. *Advances in Materials and Processing Technologies,* *6*(3), 547-564. https://doi.org/10.1080/2374068X.2020.1728645.

Ben, G., Hirabayashi, A., & Kawazoe, Y. (2013). Evaluation of quasi-isotropic plate and cylindrical shell fabricated with green composite sheets. *Advanced Composite Materials*, *22*(6), 377-387. https://doi.org/10.1080/09243046.2013.843790.

Chand, N & Fahim, M. (2020). *Tribology of natural fiber polymer composites*. Woodhead publishing, United Kingdom. ISBN: 978-0-12-818983-2(p), ISBN: 978-0-12-8189073-9(e).

Composite Materials. (n.d.). Accessed 14 April 2023 https://en.wikipedia.org/wiki/Composite_material.

Desale, G.R., Gandhi, B.K., & Jain, S.C. (2006). Effect of erodent properties on erosion wear of ductile type materials. *Wear*, *261*(7-8), 914-921. https://doi.org/10.1016/j.wear.2006.01.035.

Eldeeb, H., Midani, M., & Seyam, A.F.M. (2022). Modeling tensile behavior of 3D orthogonal woven green composites considering variability of natural fibers. *Journal of the Textile Institute*, *113*(7), 1334-1344. https://doi.org/10.1080/00405000.2021.1927938.

Hrušková, M., Bednářová, M., & Novotný, F. (2001). Wheat flour dough rheological characteristics predicted by NIRSystems 6500. *Czech Journal of Food Sciences*, *19*(6), 213-218. https://doi.org/10.17221/6610-cjfs.

Ismail, S.O., Akpan, E., & Dhakal, H.N. (2022). Review on natural plant fibres and their hybrid composites for structural applications: Recent trends and future perspectives. *Composites Part C: Open Access*, *9*, 100322. https://doi.org/10.1016/j.jcomc.2022.100322.

Jem, K.J., & Tan, B. (2020). The development and challenges of poly (lactic acid) and poly (glycolic acid). *Advanced Industrial and Engineering Polymer Research 3*(2), 60-70. https://doi.org/10.1016/j.aiepr.2020.01.002.

Jiang, D., An, P., Cui, S., Sun, S., Zhang, J., & Tuo, T. (2020). Effect of modification methods of wheat straw fibers on water absorbency and mechanical properties of wheat straw fiber cement-based composites. *Advances in Materials Science and Engineering*, *2020,* 5031025. https://doi.org/10.1155/2020/5031025.

Julias, A., (n.d.). Accessed on 11th April 2023, Volume Fraction of Composites, https://crescent.education/wp-content/uploads/2021/03/Volume-fraction-of-composites.pdf

Kim, Y.Y., Kong, H.J., & Li, V.C. (2003). Design of engineered cementitious composite suitable for wet-mixture shotcreting. *American Concrete Institute Materials Journal*, *100*(6), 511-518. https://doi.org/10.14359/12958.

Lee, J.C., Hong, Y.S., Nan, R.G., Jang, M.K., Lee, C.S., Ahn, S.H., & Kang, Y.J. (2008). Soundproofing effect of nano particle reinforced polymer composites. *Journal of Mechanical Science and Technology*, *22*(8), 1468-1474. https://doi.org/10.1007/s12206-008-0419-4.

Li, X., Sosa, M., & Olofsson, U. (2015). A pin-on-disc study of the tribology characteristics of sintered versus standard steel gear materials. *Wear*, *340-341*, 31-40. https://doi.org/10.1016/j.wear.2015.01.032.

Litwinek, D., Ziobro, R., Gambuś, H., & Sikora, M. (2016). Gluten free bread in a diet of celiacs. *International Journal of Celiac Disease*, *2*(1), 11-16. https://doi.org/10.12691/ijcd-2-1-4.

Liu, X., & Yu, W. (2006). Evaluating the thermal stability of high performance fibers by TGA. *Journal of Applied Polymer Science*, *99*(3), 937-944. https://doi.org/10.1002/app.22305.

Mangaraj, S., Yadav, A., Bal, L.M., Dash, S.K., & Mahanti, N.K. (2019). Application of biodegradable polymers in food packaging industry: A comprehensive review. *Journal of Packaging Technology and Research*, *3*(1), 77-96. https://doi.org/10.1007/s41783-018-0049-y.

Mensah, R.A., Vennström, A., Shanmugam, V., Försth, M., Li, Z., Restas, A., Neisiany, R.E., Sokol, D., Misra, M., Mohanty, A., Hedenqvist, M., & Das, O. (2022). Influence of biochar and flame retardant on mechanical, thermal, and flammability properties of wheat gluten composites. *Composites Part C: Open Access*, *9,* 100332. https://doi.org/10.1016/j.jcomc.2022.100332.

Montaño-Leyva, B., Ghizzi D. da Silva, G., Gastaldi, E., Torres-Chávez, P., Gontard, N., & Angellier-Coussy, H. (2013). Biocomposites from wheat proteins and fibers: Structure/mechanical properties relationships. *Industrial Crops and Products*, *43*, 545-555. https://doi.org/10.1016/j.indcrop.2012.07.065.

Morreale, M., Scaffaro, R., Maio, A., & La Mantia, F.P. (2008a). Effect of adding wood flour to the physical properties of a biodegradable polymer. *Composites Part A: Applied Science and Manufacturing*, *39*(3), 503-513. https://doi.org/10.1016/j.compositesa.2007.12.002.

Morreale, M., Scaffaro, R., Maio, A., & La Mantia, F.P. (2008b). Mechanical behaviour of Mater-Bi®/wood flour composites: A statistical approach. *Composites Part A: Applied Science and Manufacturing*, *39*(9), 1537-1546. https://doi.org/10.1016/j.compositesa.2008.05.015.

Muñoz, R., Rodriguez, J.A., Páez-Hernández, M.E., Sánchez-Ortega, I., & Santos, E.M. (2015). Determination of lipoxygenase activity in cereals grains using a silver nanoparticles assay. *Journal of Chemistry*, *2015*, 1-5. https://doi.org/10.1155/2015/786430.

Nyambo, C., Mohanty, A.K., & Misra, M. (2011). Effect of maleated compatibilizer on performance of PLA/Wheat straw-based green composites. *Macromolecular Materials and Engineering*, *296*(8), 710-718. https://doi.org/10.1002/mame.201000403.

Owens corning milestones, (2017.). Accessed 15th May 2022. https://www.owenscorning.com/en-us/corporate/sustainability/docs/2018/OwensCorning_2017SustainabilityReport.pdf

Perry, A.J. (1983). Scratch adhesion testing of hard coatings. *Thin Solid Films*, *107*(2), 167-180. https://doi.org/10.1016/0040-6090(83)90019-6.

Pin on Disk Test, (n.d.). Accessed on, 14 June, 2023. https://www.tribonet.org/wiki/pin-on-disk-test/.

Plastic, (n.d.). Accessed on 2nd March 2022. https://en.wikipedia.org/wiki/Plastic.

Scaffaro, R., Morreale, M., Lo Re, G., & La Mantia, F.P. (2009a). Degradation of Mater-Bi®/wood flour biocomposites in active sewage sludge. *Polymer Degradation and Stability*, *94*(8), 1220-1229 https://doi.org/10.1016/j.polymdegradstab.2009.04.028.

Scaffaro, R., Morreale, M., Lo Re, G., & La Mantia, F.P. (2009b). Effect of the processing techniques on the properties of ecocomposites based on vegetable oil-derived Mater-Bi® and wood flour. *Journal of Applied Polymer Science*, *114*(5), 2855-2863. https://doi.org/10.1002/app.30822.

Shewry, P.R. (2009). The HEALTHGRAIN programme opens new opportunities for improving wheat for nutrition and health. *Nutrition Bulletin*, *34*(2), 225-231. https://doi.org/10.1111/j.1467-3010.2009.01747.x.

Schwartz M.M. (1992). *Composite materials handbook*. McGraw hill.

Taib, N.A.A.B., Rahman, M.R., Huda, D., Kuok, K.K., Hamdan, S., Bakri, M.K.B., Julaihi, M.R.M.B., & Khan, A. (2023). A review on poly lactic acid (PLA) as a biodegradable polymer. *Polymer Bulletin*, *80*(2), 1179-1213. https://doi.org/10.1007/s00289-022-04160-y.

Technical specifications test setup screen test graph showing normal load and tangential force (Ft), (n.d.). Accessed on 15th June 2023. www.ducom.com. Retrieved from https://www.dora-tec.com/images/ stories/ pdf/ ducom%20tr-101%20scratch%20tester%20eng.pdf.s

Thermo-gravimetric analysis, (n.d.). Accessed on 15th May 2022. https://en.wikipedia.org/wiki/Thermo-gravimetric_analysis.

Tobias P.H., Völker, C., Kramm, J., Landfester, K., Wurm, F.R. (2018). Plastics of the future the impact of biodegradable polymers on the environment and on society. https://onlinelibrary.wiley.com/doi/10.1002/anie.201805766.

Yadav, M., Kumaraswamidhas, L.A., & Singh, S.K. (2022). Investigation of solid particle erosion behavior of Al-Al_2O_3 and Al-ZrO_2 metal matrix composites fabricated through powder metallurgy technique. *Tribology International*, *172*, 107636. https://doi.org/10.1016/j.triboint.2022.107636.

Publisher's Note- Ram Arti Publishers remains neutral regarding jurisdictional claims in published maps and institutional affiliations.